

**PHS PUBLIC ACCESS**

Author manuscript

IEEE Sens J. Author manuscript; available in PMC 2015 September 25.

Published in final edited form as:

IEEE Sens J. 2013 November 1; 13(11): 4534–4541. doi:10.1109/JSEN.2013.2270008.

**Detection and Monitoring of Microparticles Under Skin by Optical Coherence Tomography as an Approach to Continuous Glucose Sensing Using Implanted Retroreflectors****Shang Wang,**

Department of Biomedical Engineering, University of Houston, Houston, TX 77204 USA.

**Tim Sherlock,**

Department of Electrical and Computer Engineering, University of Houston, Houston, TX 77204 USA.

**Betsy Salazar,**

Department of Biomedical Engineering, University of Houston, Houston, TX 77204 USA.

**Narendran Sudheendran,**

Department of Biomedical Engineering, University of Houston, Houston, TX 77204 USA.

**Ravi Kiran Manapuram,**

Department of Mechanical Engineering, University of Houston, Houston, TX 77204 USA. He is now with Biotigen Inc., Morrisville, NC 27560 USA.

**Katerina Kourentzi,**

Department of Chemical and Biomolecular Engineering, University of Houston, TX 77204 USA.

**Paul Ruchhoeft [Member, IEEE],**

Department of Electrical and Computer Engineering, University of Houston, Houston, TX 77204 USA.

**Richard C. Willson, and**

Department of Chemical and Biomolecular Engineering, University of Houston, TX 77204 USA, and also with the Methodist Hospital Research Institute, Houston, TX 77031 USA.

**Kirill V. Larin [Member, IEEE]**

Department of Biomedical Engineering, University of Houston, Houston, TX 77204 USA, and also with the Department of Molecular Physiology and Biophysics, Baylor College of Medicine, Houston, TX 77030 USA.

**Abstract**

We demonstrate the feasibility of using optical coherence tomography (OCT) to image and detect 2.8  $\mu\text{m}$  diameter microparticles (stationary and moving) on a highly-reflective gold surface both in clear media and under skin *in vitro*. The OCT intensity signal can clearly report the microparticle count, and the OCT response to the number of microparticles shows a good linearity. The detect

ability of the intensity change ( $2.9\% \pm 0.5\%$ ) caused by an individual microparticle shows the high sensitivity of monitoring multiple particles using OCT. An optical sensing method based on this feasibility study is described for continuously measuring blood sugar levels in the subcutaneous tissue, and a molecular recognition unit is designed using competitive binding to modulate the number of bound microparticles as a function of glucose concentration. With further development, an ultra-small, implantable sensor might provide high specificity and sensitivity for long-term continuous monitoring of blood glucose concentration.

## Keywords

Biomedical monitoring; magnetic microparticles; optical coherence tomography; skin; retroreflection

---

## I. Introduction

Frequent blood glucose monitoring is highly recommended for patients suffering from diabetes in order to prevent acute complications and reduce the risk of long-term problems [1]. However, the most widely used current sensing method requires collection of a droplet of blood from a fingertip through a puncture, which is painful and uncomfortable and acts as a deterrent to frequent blood glucose measurements. To improve management of diabetes and make blood glucose testing easier and less painful, an implantable (or noninvasive) sensor, capable of providing continuous measurement of blood glucose levels, offers the opportunity for improved therapeutic interventions [2], [3].

Both electrochemical and optical methods have been extensively studied as possible approaches to an implantable (noninvasive) glucose sensor. Owing to concerns for potential leaching of mediators, the majority of implantable sensors applying electrochemical methods are based on the irreversible oxidation of glucose [4]. Most electrochemical sensors have issues of biocompatibility, short storage and operational lifetimes, and response drift [4], [5]. Optical methods based on the measurement of photons interacting with tissues have certain advantages, such as being free of a reference electrode and consumable reagents, and being capable of sterile remote sensing and multiplexing [5], [6]. Optical glucose sensing methods can be divided into two broad categories: one approach is to measure the direct effects of glucose molecules on the properties of light (e.g. intensity and polarization), and the other is to use a molecular recognition technique to transduce the glucose concentration into a detectable light signal. Both of these methods have the potential to be developed as a noninvasive or implantable optical sensor.

Several optical techniques have been proposed for noninvasive blood glucose sensing [6]–[8]. Near-infrared (NIR) spectroscopy provides information on glucose concentration by measuring the transmission or reflectance of light. As glucose can alter optical absorption properties of tissues, changes in the transmission or reflectance spectrum can be linked to the changes in blood glucose concentration [9], [10]. However, the tissue absorption coefficient also depends on factors such as temperature and changes in the concentration of other analytes, which highly affects the accuracy of sensing. Raman spectroscopy derives an estimation of glucose concentration through analysing the scattered light influenced by the

oscillation and rotation of glucose molecules [11], [12]. Although the Raman spectrum of glucose is well differentiable from that of other molecules, the long spectral acquisition time and the presence of many other unrelated compounds can strongly limit the clinical application of this method. Polarimetry utilizes the optical rotatory dispersion of glucose molecules and reflects the blood glucose concentration by measuring the change of the polarization plane of linearly polarized light [13], [14]. An anatomic location suggested to be well suited for the polarimetric measurement is the anterior chamber of the eye, as the scattering of light in the eye is generally very small compared with other types of tissues. Problems of this method mainly exist in the interference related to the optical rotation effects from the cornea and other optically active components in the aqueous humour. Optical coherence tomography (OCT) allows depth-resolved assessment of tissue scattering coefficient (which is altered by the changes of glucose concentration) using a low coherence interferometer [15]–[18]. But, similar to NIR spectroscopy, varying physiological and environmental conditions could also alter the scattering properties of tissue, which highly affects the measurement accuracy.

To improve specificity, a major effort has been focused on designing and implementing a glucose recognition and reporting unit which can be implanted under the skin and provide a detectable light property change caused by the variation of glucose concentration. Methods including kinetic enzymatic assays using glucose oxidation [19], [20], chemical binding of glucose to synthetic boronic acid [21], [22], affinity binding to Concanavalin A (Con A) [23]–[25], and affinity binding to glucose binding proteins [26], [27] have been studied and combined with fluorescence, scattering and fiber optic techniques for blood glucose sensing. Glucose recognition utilizing affinity binding to Con A offers certain advantages, including full reversibility, feasibility of calibration, weak pH-dependence, and no effect of varying oxygen partial pressure [5]. Con A is a plant lectin which has four binding sites for glucose and carbohydrates (e.g. dextran). Since it was first explored by Schultz *et al.* using fluorescence detection [23], [24], the application of this method has been extensively studied with fluorescence labelling and imaging techniques to improve the glucose sensing ability with high specificity [25], [28]–[31]. However, nonspecific changes in fluorescence reduce the glucose sensing accuracy and reliability.

Recently, Ballerstadt *et al.* investigated the feasibility of using OCT to monitor the turbidity of an implantable glucose recognition unit in order to analyse the glucose concentration [32]. The turbidity change is induced by glucose binding to Con A. The glucose-specific scattering sensitivity can reach up to 7%  $\text{mM}^{-1}$  when measured in air, and remains 0.26%  $\text{mM}^{-1}$  when tested in a tissue phantom. However, this sensing method may not be able to maintain sensing specificity and accuracy when implemented below skin due to the large attenuation of the OCT signals from tissue. Also, the aggregation of free Con A will shorten the sensor's potential lifetime. Thus, for the purpose of developing highly specific implantable glucose sensing method with enhanced sensitivity and long operation time, we propose a glucose recognition unit with microparticles-labelled dextran and a highly-reflective gold mirror coated with Con A. The gold mirror surface is used to provide a strong reflection signal for maintaining sufficient sensing accuracy after implantation (for the final construction, we intend to utilize a micro-retroreflector-based gold platform [33], which is

able to provide high contrast for the detection of reflected light within tissue). The immobilization of Con A on the gold mirror surface greatly reduces its aggregation rate and therefore extends the effective sensing lifetime. For housing the unit, a semi-permeable membrane can be applied to allow free diffusion of glucose molecules while being impermeable to cells and microparticles. A schematic of the proposed structure is shown in Figure 1. Glucose recognition is realized by competitive displacement of glucose and microparticles-labelled dextran to Con A. With different glucose concentration, the binding competition of glucose and dextran to Con A will modulate the microparticle density within the imaging area on the gold mirror surface. Due to the reversible property of competitive binding [34], specifically, lower glucose concentration will enable more microparticles to be localized on the surface, and increasing glucose concentration will reduce the amount of microparticles. Therefore, through monitoring the number of microparticles within the target area, glucose concentration can be determined. For continuous glucose monitoring, the sensing unit is expected to be implanted in the upper layer of the dermis, located approximately 150–300  $\mu\text{m}$  from the skin surface (illustrated in Figure 1).

More recently, we have demonstrated that OCT has the capability of depth-resolved imaging of highly-reflective micro-structures under tissue up to 910  $\mu\text{m}$  in depth [35], and, thus, OCT could be used to detect the change of the reflection of light from a gold mirror surface under tissue and to monitor the microparticle number based on the scattering properties of these particles. Since we expect that the glucose concentration can be well represented by the amount of bound microparticles, the sensitivity and specificity of the proposed sensing system are highly dependent on how well the microparticles can be resolved by OCT and how well the signal from OCT and the microparticle density are correlated. In this paper, we show results from a feasibility study where we focused on the quantification of the reflection variation caused by the change of microparticle number on a mirrored surface and also the monitoring of the microparticles both in clear media and under skin tissue using OCT.

## II. Materials and Methods

### A. Microparticles

For the proposed sensing method, the microparticles should be small in size, easy to manipulate, and able to be coated with dextran. Thus, our primary selection focused on Dynabeads with carboxylic acid groups (Life Technologies Corporation). Two available sizes with 1.05  $\mu\text{m}$  and 2.8  $\mu\text{m}$  diameter are suitable for the construction of the sensing unit. Also, their superparamagnetic property allows the use of magnets to control the microparticles' position within the capsule. It is well known that the attenuation of the light is dependent, among others, on the diameter of the scatters and the wavelength of the light [36]. Typically OCT employs the central wavelengths around 800 nm and 1300 nm [37]. Thus, we performed a preliminary study of light attenuation versus microparticle concentrations using two OCT systems with the laser sources around these wavelengths. Fig. 2 shows the dependence of the attenuation coefficient on microparticle concentrations for the 1.05  $\mu\text{m}$  and the 2.8  $\mu\text{m}$  diameter microparticles using OCT system centered at 840 nm and 1325 nm. A linear fit was applied to the data to quantify the slope of the change, and it can be seen that, in Fig. 2(c), the change of attenuation coefficient appears to have the

highest slope. Moreover, for the low concentration range (200 particles/nL), the slope in Fig. 2(c) is even steeper. This result indicates the sensitivity of the attenuation coefficient to the changes in microparticle number is greatest for microparticles with 2.8  $\mu\text{m}$  in diameter at a central wavelength of 840 nm. Thus, based on this test, Dynabeads M-270 Carboxylic Acid (2.8  $\mu\text{m}$  diameter) was chosen for the feasibility study of the proposed sensing method.

## B. OCT System and en Face OCT Imaging

A spectral domain OCT system with the central wavelength of 840 nm was chosen for use in this study based on the preliminary data described in Fig. 2. The schematic of the system is shown in Fig. 3. The laser source (superluminescent diode) has a bandwidth of  $\sim 49$  nm with the output power of around 20 mW. The OCT system is based on a Michelson interferometer where the light from the reference and the sample arms interference. A home-built spectrometer is utilized to resolve the wavelengths and detect the interference fringes. In the spectrometer, the collimated beam falls onto a 1200 l/mm holographic transmission grating, and the beam with spatially-separated wavelengths is focused onto the 2048 pixels of a CCD. The data acquisition from the CCD is synchronized with the Galvo mirrors in the sample arm that are used for the two-dimensional transverse scan of the sample. The A-line (depth-resolved imaging) speed of the OCT system can reach up to 29 kHz. An axial resolution of  $\sim 12$   $\mu\text{m}$  (in air) and a transverse resolution of  $\sim 8$   $\mu\text{m}$  can be achieved. The maximum imaging depth in scattering tissues (assuming refractive index of 1.4) is around 3 mm.

The position of the gold mirror surface can be located and selected from the depth-resolved OCT images and the intensity of the OCT signal at this particular depth represents the reflection from the gold mirror surface. Because the light scattering from the microparticles reduces the intensity of the localized reflected light from the gold mirror surface, an *en face* OCT image with the information of reflection shows the microparticle distribution across the gold mirror surface.

## C. Gold Mirror

To create gold mirror surfaces, 100 mm diameter silicon wafers were coated with a 10 nm thick layer of titanium followed by a 100 nm thick layer of gold deposited using thermal evaporation.

## D. Mouse Ear

Skin from a mouse ear was used in the *in vitro* studies. A mouse ear was dissected and kept in 0.9% saline before experiments. During experiments, distilled water was added to avoid dehydration. Based on the measurement from OCT three-dimensional images, the skin tissue from the mouse ear had a thickness of 150–300  $\mu\text{m}$ .

## E. Experimental Procedure

The experiments for the feasibility study of the proposed glucose sensing method were performed in three phases.

- 1) Assessing the variation of intensity from OCT signal with the change of microparticle number on the gold mirror surface. Low-concentration ( $1 \times 10^3$  particles/ $\mu\text{L}$  –  $1 \times 10^5$  particles/ $\mu\text{L}$ ) microparticle solutions were prepared and deposited on the surface of gold mirrors. The mirrors were marked with cross-shaped scratches to provide reference positions. After the microparticles were allowed to dry on the gold mirror, an optical microscope and the OCT system were used to image the same regions. The mapping of the microparticles on the gold mirror surface using *en face* OCT images was examined by the corresponding microscope images. Based on the mapping results, the change of intensity from OCT signal at the microparticle locations was quantified.
- 2) Imaging and detecting the movement of microparticles in clear media. A low-concentration microparticle solution (1 mL, 200 particles/ $\mu\text{L}$ ) was prepared and deposited on the gold mirror surface of  $\sim 172 \text{ mm}^2$  area. The microparticles settled on the mirror surface before the OCT recording was started. The OCT imaging area was set to be  $935 \times 187 \mu\text{m}^2$  with a scanning interval of  $\sim 2.3 \mu\text{m}$ . The imaging speed was 2 seconds per two-dimensional scan. A magnetic field was applied at the time around 3.5 minutes after the recording started. The average of the intensity of OCT signal from the gold mirror surface in each two-dimensional scan was obtained and recorded over time. Also, *en face* OCT images at different time points were generated.
- 3) Detecting and monitoring the movement of microparticles under skin tissue *in vitro*. The skin tissue from a mouse ear was placed on the gold mirror, and a microparticle solution of 200 particles/ $\mu\text{L}$  was added between the tissue and the gold mirror surface, forming a layer with a thickness of about 0.7–1.0 mm. The experimental setup is shown with a picture in Fig. 4(a). An area of  $935 \times 187 \mu\text{m}^2$  was scanned by the OCT system, and a typical three-dimensional OCT image, including the gold mirror surface and the skin tissue, is shown in Fig. 4(b). The OCT transverse scanning interval was also kept at  $\sim 2.3 \mu\text{m}$  and the recording time for each two-dimensional scan was 2 seconds. Similar to the second phase, the average of the intensity of OCT signal from the gold mirror surface in each two-dimensional scan was plotted over time for both before and after applying the magnetic field.

### III. Results and Discussions

Selected typical *en face* OCT images of microparticles deposited on the gold mirror surface are shown in Fig. 5(a) and (c). The corresponding optical microscope images of the same imaging regions are shown in Fig. 5(b) and (d). The locations of the cross-shaped scratches offered the references for the mapping of the microparticles. Fig. 5 shows that OCT is able to correctly map the distribution of microparticles on the gold mirror surface. The clusters of three microparticles and the corresponding dark points in the *en face* OCT images are called out with the black arrows in Fig. 5.

By mapping the intensity signals from the OCT scan to the actual microparticle count, the fractional decrease in the intensity of OCT signal was calculated for single microparticles

and aggregates containing a variety of microparticle counts. The result is shown in Fig. 6. For single microparticles and aggregates with 2–8 microparticles,  $N = 4$  (samples for measurement). Since the aggregates with more microparticles are rare, for aggregates with 9, 10 and 11 microparticles,  $N = 1$  (sample for measurement). Fig. 6 shows that when the number of microparticles increases, the intensity decreases with an approximately linear ( $R = 0.89$ ) relationship. The intensity change caused by one single microparticle is  $2.9\% \pm 0.5\%$ . These results indicate that OCT has the ability to assess the microparticle number through detecting the change of local reflection. Also, the detectable individual microparticle with an intensity decrease of  $2.9\% \pm 0.5\%$  suggests a high sensitivity of using OCT to identify single microparticle on the gold mirror surface.

In the next experiments, we investigated the feasibility of using OCT to detect the movement of microparticles through both clear media and skin tissue *in vitro*. Fig. 7 shows the typical result from the experiments of monitoring microparticles through water. The intensity information of the OCT signal from the gold mirror surface can represent the state of the microparticles within the scanning region. The intensity (averaged from two-dimensional scanning area) detected from the gold mirror surface covered with only water was first recorded and used as the reference value for normalization. From Fig. 7(a), it can be seen that during the time range of 0–3.5 minutes, the signal has a relatively high frequency and small amplitude of variation, which we attribute to the Brownian motion of the microparticles in water. When a magnetic field is applied at about 3.5 minutes into the experiment, the microparticles start to form long chains (similar as the phenomenon observed in [38]) and move into the direction of the magnet, which can be observed in Fig. 7(b) and (c). As the microparticles are pulled out from the scanning region, shown in Fig. 7(c), (d) and (e), the intensity signal increases over time, and remains relatively constant after about 14 minutes. During the time of 14–17 minutes, the left several clusters of microparticles cannot be moved by the magnetic field and maintain stable on the gold mirror surface, as shown in Fig. 7(f) and (g). The fluctuation of the intensity signal during different periods in the experiment is analyzed in Fig. 7(h). For each period, the percentage of the signal fluctuation was calculated with the standard deviation of the normalized intensity divided by the relevant averaged value. From Fig. 7(h), it can be seen that the fluctuation of the signal from 0–3.5 minutes and 14–17 minutes is much smaller than the one during 3.5–14 minutes when the magnetic field was just applied to the microparticles. This is because large amounts of microparticles in clusters were driven out of and also into the scanning region from the time of 3.5–14 minutes, which resulted in the signal fluctuation with relatively very high amplitude and low frequency, as shown in Fig. 7(a). It can also be observed that the fluctuation of the signal during 14–17 minutes appears to be half smaller than the one during 0–3.5 minutes. This can be explained by the fact that during the last three minutes, there were fewer microparticles present in the scanning region, which indicates the overall Brownian motion of the microparticles during this period is much less than the one during the time of 0–3.5 minutes. These results indicate that the state of microparticles on the gold mirror surface can be clearly monitored over time through clear media based on the intensity information of the OCT signal.

The result from the experiment of detecting the movement of microparticles under skin tissue *in vitro* is presented in Fig. 8. The averaged intensity value from each two-dimensional scan is plotted over time to represent the state of microparticles under tissue before and after applying the magnetic field. Similar to the result presented in Fig. 7, during 0–2 minutes (before the magnetic field was applied), the variation of the intensity signal appears to have lower amplitude and higher frequency relative to the one from the time of 2–4 minutes when the magnetic field was applied, as shown in Fig. 8(a). This is caused by the movement of microparticle clusters over the scanning region. Also, similarly, it can be observed that the averaged intensity increases to a higher value after the magnetic field was applied, due to fewer microparticles remaining within the scanning region. These are also indicated in Fig. 8(b) where the intensity signals are compared before and after applying the magnetic field. The percentage of the signal fluctuation has been calculated to be 0.6% and 1.0% for the time periods before and after the magnetic field was applied, respectively. This is comparable with the data presented in Fig. 7(h). The differences (0.6% to 0.4% and 1.0% to 1.5%) can be a result of the variation of the light scattering from skin tissue over the monitoring period. The result presented in Fig. 8 demonstrates that OCT can be utilized to detect the movement of microparticles over time on the gold mirror surface under skin tissue *in vitro*.

These results from the feasibility study belong to the first phase in our goal of developing optical implantable sensing method to continuously monitor the blood sugar levels in the subcutaneous tissue. The disadvantage of using gold mirror lies in the challenges to position the gold mirror surface perpendicular to the laser beam as well as to maintain exactly the same scanning region during multiple times of measurements. Regarding this problem, a micro-retroreflector-based gold platform with a fixed distribution pattern has been designed and manufactured to provide highly-reflected light and also the possibility of implantation [33]. For the imaging with OCT, the platform has been demonstrated to be able to offer well-specified region and good signal-to-noise ratio [35].

The proposed glucose sensing method consists of two information-transducing steps. The first one is from the glucose concentration to the number of microparticles through a competitive displacement process, and the second one is from the microparticle number to the intensity of OCT signal. The presented results focus on the latter step and have demonstrated the feasibility of using OCT to detect and monitor microparticles on the gold mirror surface both in clear media and under skin tissue *in vitro*. Based on our recent preliminary experiments using micro-channels, we have also observed that the dextran-coated microparticles with a diameter of  $\sim 3 \mu\text{m}$  bind efficiently onto the gold surface that is functionalized with Con A. Additionally, the presence of glucose results in a decrease in the number of bound microparticles on the gold surface due to a reduction in the number of available binding sites on the Con A-functionalized surface. In the future, our work will focus on optimizing the chemistry for sensing glucose. We also plan to integrate our approach with micro-retroreflector-based sensing elements and to investigate the relationship between the OCT intensity signal and the glucose concentration.



## IV. Conclusion

We describe the concept of a new optical glucose sensing method for continuous monitoring blood sugar levels in the upper dermis layer. The method is based on the competitive binding of glucose and microparticles-labelled dextran to Con A immobilized on the surface of a highly-reflective implantable gold platform. With the reversible binding process, an increase in glucose concentration reduces the amount of microparticles within the target region on the gold mirror surface. Due to the light scattering property of microparticles, the information of microparticle number can be revealed by detecting the change of light reflection from the gold mirror surface using OCT. The diameter of the microparticles and the central wavelength of OCT system are optimized for the sensitivity of the detection. The feasibility of using OCT to detect and monitor the microparticles on the gold mirror surface has been demonstrated both in clear media and through skin tissue *in vitro*. The detectable intensity change of  $2.9\% \pm 0.5\%$  caused by an individual microparticle suggests a high sensitivity of microparticle detection using OCT. With further development, the proposed method can potentially offer improved sensitivity and convenience for the everyday blood glucose monitoring.

## Acknowledgments

This work was supported in part by the National Science Foundation under Grant CMMI-0900743, the Welch Foundation under Grant E-1264, and the NIAID/NIH under Grant U54 AI057156. The associate editor coordinating the review of this paper and approving it for publication was Prof. E. H. Yang.

## Biography



**Shang Wang** is currently pursuing the Ph.D. degree in biomedical engineering at the University of Houston, Houston, TX, USA. He received the bachelor's degree in optoelectronic information engineering from the Harbin Institute of Technology, Harbin, China, in 2010. His current research interests include biomedical optics, with the current focus on the development of optical coherence tomography and elastography methods for tissue characterization and biomedical sensing.



**Tim Sherlock** received the B.S. degree in engineering science from Trinity University, San Antonio, TX, USA, in 2006, and the Ph.D. degree in electrical engineering from the University of Houston, Houston, TX, USA, in 2011, working on the fabrication of micro retroreflectors for use in optical biosensors. His current research interests include nanofabrication techniques, specifically novel lithography and etching processes.



**Betsy Salazar** is currently pursuing the Ph.D. degree in biomedical engineering at the University of Houston, Houston, TX, USA. She received the bachelor's degree in biomedical engineering from the University of Houston in 2011. Her current research interests include cardiovascular tissue engineering, with the current focus of engineering cardiac tissues and enhancing their performance with electrical, mechanical, and perfusion bioreactors.



**Narendran Sudheendran** is currently pursuing the Ph.D. degree in biomedical engineering at the University of Houston, Houston, TX, USA. He received the M.S. degree in electrical engineering from the University of Houston in 2010. His current research interests include designing algorithms and software tools to study the morphological features especially that of the cardiovascular system during the development of mouse embryo imaged using optical coherence tomography.



**Ravi Kiran Manapuram** is currently a Development Engineer with the Department of Research and Development, Bioptigen, Inc., Morrisville, NC, USA. He received the M.S. degree in electrical engineering and the Ph.D. degree in mechanical engineering from the University of Houston, Houston, TX, USA, in 2008 and 2012, respectively. His current research interests include developing systems for noninvasive and nondestructive imaging and diagnostics of tissues and cells. He has authored 14 peer-reviewed publications and has received numerous awards, including Research Excellence Award from SPIE, selected under top 50 optics researchers by the Nanobiophotonics Summer School Organized by University of Illinois at Urbana Champagne, Appreciation Award for active participation in an organizing committee for ECE graduate research conference at University of Houston. He has delivered eight talks in various conferences.



**Katerina Kourentzi** is a Research Assistant Professor of chemical and biomolecular engineering with the University of Houston, Houston, TX, USA. She received the Diploma degree in chemical engineering from National Technical University, Athens, Greece, in 1996, and the Ph.D. degree in chemical engineering from the University of Houston in 2002. Her current research interests include the interface of engineering and biotechnology, the development of ultra sensitive detection labels and reporters and their application in diagnostic assays for the early diagnosis of disease.



**Paul Ruchhoeft** is an Associate Professor of electrical and computer engineering with the University of Houston, Houston, TX, USA, where he joined as the Faculty Member in 2001. He received the B.S. degree in electrical engineering from the University of Texas at Austin, Austin, TX, USA, in 1995, and the M.S. and Ph.D. degree from the University of Houston in

1998 and 2000, respectively. His research lies in the areas of nanolithography and nanofabrication, where he develops high-resolution, parallel printing processes using helium ions and atoms and the associated processes. His current research interests include using these patterning techniques to develop complex systems. He is the author of more than 35 publications, holds eight patents, and has presented his findings through more than 60 research presentations.



**Richard C. Willson** is a John and Rebecca Moores Professor of chemical and biomolecular engineering, biology and biochemistry, and biomedical engineering with the University of Houston, Houston, TX, USA. He holds joint appointments with the Methodist Hospital Research Institute, Houston, and in the SCBMB Program, Baylor College of Medicine, and serves as a Diagnostics Theme Leader of the NIH Western Regional Center of Excellence. He received the B.S. (Hons.) and M.S. degrees in chemical engineering from the California Institute of Technology, Pasadena, CA, USA, and the Ph.D. degree in chemical engineering and post-doctoral studies in biology from the Massachusetts Institute of Technology, Cambridge, MA, USA. His current research interests include molecular recognition and its applications in diagnostics and bioseparations. He is a recipient of the NSF PYI and NIH FIRST Awards, and a Fellow of the AIMBE and AAAS.



**Kirill V. Larin** is an Associate Professor of biomedical engineering with the University of Houston, Houston, TX, USA. He also holds joint appointments with the Department of Physiology and Biophysics, Baylor College of Medicine and Department of Optics and Biophysics, Saratov State University, Saratov, Russia. He received the first M.S. degree in laser physics and mathematics from Saratov State University in 1995, the second M.S. degree in cellular physiology and molecular biophysics in 2001, and the Ph.D. degree in biomedical engineering from the University of Texas Medical Branch, Galveston, TX, USA, in 2002. His research contributions are in biomedical optics and biophotonics and development and application of various optical methods for noninvasive and nondestructive imaging and diagnostics of tissues and cells. He has authored more than 70 peer-reviewed publications and chapters in six books on *Biomedical Optics*. He has received numerous awards, including the Presidential Award from Russian President Boris Yeltsin, the Wallace

Coulter Young Investigator Translation Award, the Office of Naval Research Young Investigator Award, the Outstanding Young Investigator Award from the Houston Society for Engineers in Medicine and Biology, and the Herbert Allen Award from American Society for Mechanical Engineers. He has delivered more than 50 invited and plenary talks, serves as a Chair of Dynamics and Fluctuations in Biomedical Photonics and Optical Elastography conferences and a member of number technical committees at professional conferences. He is an Instructor for short courses on Tissue Optics and Biophotonics for the SPIE, IEEE, and OSA.

## References

1. Association AD. Standards of medical care in diabetes-2011. *Diabetes Care*. 2011; 34(1):S11–S61. [PubMed: 21193625]
2. Burge MR, Mitchell S, Sawyer A, Schade DS. Continuous glucose monitoring: The future of diabetes management. *Diabetes Spectr*. 2008; 21(2):112–119.
3. Wilson GS, Gifford R. Biosensors for real-time in vivo measurements. *Biosens. Bioelectron*. 2005; 20(12):2388–2403. [PubMed: 15854814]
4. Wang J. Electrochemical glucose biosensors. *Chem. Rev*. 2007; 108(2):814–825. [PubMed: 18154363]
5. Steiner M-S, Duerkop A, Wolfbeis OS. Optical methods for sensing glucose. *Chem. Soc. Rev*. 2011; 40(9):4805–4839. [PubMed: 21674076]
6. McNichols R, Coté G. Optical glucose sensing in biological fluids: An overview. *J. Biomed. Opt*. 2000; 5(1):5–16. [PubMed: 10938760]
7. Tura A, Maran A, Pacini G. Non-invasive glucose monitoring: Assessment of technologies and devices according to quantitative criteria. *Diabetes Res. Clinical Pract*. 2007; 77(1):16–40. [PubMed: 17141349]
8. Khalil OS. Non-invasive glucose measurement technologies: An update from 1999 to the dawn of the new millennium. *Diabetes Technol. Therapeutics*. 2004; 6(5):660–697.
9. Malin SF, Ruchti TL, Blank TB, Thennadil SN, Monfre SL. Noninvasive prediction of glucose by near-infrared diffuse reflectance spectroscopy. *Clinical Chem*. 1999; 45(9):1651–1658. [PubMed: 10471679]
10. Amerov AK, Chen J, Small GW, Arnold MA. Scattering and absorption effects in the determination of glucose in whole blood by near-infrared spectroscopy. *Anal. Chem*. 2005; 77(14):4587–4594. [PubMed: 16013877]
11. Yonzon CR, Haynes CL, Zhang X, Van Duyne RP. A glucose biosensor based on surface-enhanced raman scattering: Improved partition layer, temporal stability, reversibility, and resistance to serum protein interference. *Anal. Chem*. 2003; 76(1):78–85. [PubMed: 14697035]
12. Hanlon EB, Manoharan R, Koo TW, Shafer KE, Motz JT, Fitzmaurice M, Kramer JR, Itzkan I, Dasari RR, Feld MS. Prospects for in vivo Raman spectroscopy. *Phys. Med. Biol*. 2000; 45(2):R1–59. [PubMed: 10701500]
13. Rabinovitch B, March WF, Adams RL. Noninvasive glucose monitoring of the aqueous humor of the Eye: Part I. Measurement of very small optical rotations. *Diabetes Care*. 1982; 5(3):254–258. [PubMed: 7172992]
14. Rawer R, Stork W, Kreiner CF. Non-invasive polarimetric measurement of glucose concentration in the anterior chamber of the eye. *Graefe's Archive Clinical Experim. Ophthalmol*. 2004; 242(12):1017–1023.
15. Larin KV, Eledrisi MS, Motamedi M, Esenaliev RO. Non-invasive blood glucose monitoring with optical coherence tomography. *Diabetes Care*. 2002; 25(12):2263–2267. [PubMed: 12453971]
16. Esenaliev RO, Larin KV, Larina IV, Motamedi M. Non-invasive monitoring of glucose concentration with optical coherence tomography. *Opt. Lett*. 2001; 26(13):992–994. [PubMed: 18040511]

17. Kholodnykh AI, Petrova IY, Larin KV, Motamedi M, Esenaliev RO. Precision of measurement of tissue optical properties with optical coherence tomography. *Appl. Opt.* 2003; 42(16):3027–3037. [PubMed: 12790454]
18. Larin KV, Motamedi M, Ashitkov TV, Esenaliev RO. Specificity of noninvasive blood glucose sensing using optical coherence tomography technique: A pilot study. *Phys. Med. Biol.* 2003; 48(10):1371–1390. [PubMed: 12812453]
19. Sierra JF, Galbán J, Castillo JR. Determination of glucose in blood based on the intrinsic fluorescence of glucose oxidase. *Anal. Chem.* 1997; 69(8):1471–1476.
20. De Luca P, Lepore M, Portaccio M, Esposito R, Rossi S, Bencivenga U, Mita DG. Glucose determination by means of steady-state and time-course UV fluorescence in free or immobilized glucose oxidase. *Sensors.* 2007; 7(11):2612–2625.
21. James TD, Sandanayake KRAS, Shinkai S. Novel photoinduced electron-transfer sensor for saccharides based on the interaction of boronic acid and amine. *J. Chem. Soc., Chem. Commun.* Jan.1994 4:477–478.
22. Eggert H, Frederiksen J, Morin C, Norrild JC. A new glucose-selective fluorescent bisboronic acid. first report of strong  $\alpha$ -Furanose complexation in aqueous solution at physiological pH1. *J. Organic Chem.* 1999; 64(11):3846–3852.
23. Schultz, JS. Optical sensor of plasma constituents. 1982. U.S. Patent 4344438
24. Schultz JS, Mansouri S, Goldstein IJ. Affinity sensor: A new technique for developing implantable sensors for glucose and other metabolites. *Diabetes Care.* 1982; 5(3):245–253. [PubMed: 6184210]
25. Mansouri S, Schultz JS. A miniature optical glucose sensor based on affinity binding. *Nat. Biotechnol.* 1984; 2(10):885–890.
26. Champdor M, Staiano M, Aurilia V, Stepanenko OV, Parracino A, Rossi M, D'Auria S. Thermostable proteins as probe for the design of advanced fluorescence biosensors. *Rev. Environ. Sci. Biotechnol.* 2006; 5(2–3):233–242.
27. Sakaguchi-Mikami A, Taneoka A, Yamoto R, Ferri S, Sode K. Engineering of ligand specificity of periplasmic binding protein for glucose sensing. *Biotechnol. Lett.* 2008; 30(8):1453–1460. [PubMed: 18414800]
28. Ballerstadt R, Evans C, McNichols R, Gowda A. Concanavalin A for in vivo glucose sensing: A biotoxicity review. *Biosens. Bioelectron.* 2006; 22(2):275–284. [PubMed: 16488598]
29. Ballerstadt R, Schultz JS. A fluorescence affinity hollow fiber sensor for continuous transdermal glucose monitoring. *Anal. Chem.* 2000; 72(17):4185–4192. [PubMed: 10994982]
30. Ballerstadt R, Polak A, Beuhler A, Frye J. In vitro long-term performance study of a near-infrared fluorescence affinity sensor for glucose monitoring. *Biosens. Bioelectron.* 2004; 19(8):905–914. [PubMed: 15128110]
31. Ballerstadt R, Evans C, Gowda A, McNichols R. In vivo performance evaluation of a transdermal near- infrared fluorescence resonance energy transfer affinity sensor for continuous glucose monitoring. *Diabetes Technol. Therapeutics.* 2006; 8(3):296–311.
32. Ballerstadt R, Kholodnykh A, Evans C, Gowda A, Boretsky A, McNichols R. Affinity-based turbidity sensor for glucose monitoring by optical coherence tomography: Toward the development of an implantable sensor. *Anal. Chem.* 2007; 79(18):6965–6974. [PubMed: 17702528]
33. Sherlock T, Nasrullah A, Litvinov J, Cacao E, Knoop J, Kemper S, Kourentzi K, Kar A, Ruchhoeft P, Willson R. Suspended, micron-scale corner cube retroreflectors as ultra-bright optical labels. *J. Vacuum Sci. Technol. B, Microelectron. Nanometer Struct.* 2011; 29(6):06FA01–1–06FA01-5.
34. Gestwicki JE, Cairo CW, Strong LE, Oetjen KA, Kiessling LL. Influencing receptor-ligand binding mechanisms with multivalent ligand architecture. *J. Amer. Chem. Soc.* 2002; 124(50): 14922–14933. [PubMed: 12475334]
35. Ivers SN, Baranov SA, Sherlock T, Kourentzi K, Ruchhoeft P, Willson R, Larin KV. Depth-resolved imaging and detection of micro-retroreflectors within biological tissue using optical coherence tomography. *Biomed. Opt. Exp.* 2010; 1(2):367–377.
36. Tuchin, VV. *Soc. Opt. Eng. SPIE/Int; Bellingham, WA, USA: 2007. Tissue Optics: Light Scattering Methods and Instruments for Medical Diagnosis..*

37. Schmitt JM. Optical coherence tomography (OCT): A review. *IEEE J. Sel. Topics Quantum Electron.* Jul.1999 5(4):1205–1215.
38. Park SY, Handa H, Sandhu A. Magneto-optical biosensing platform based on light scattering from self-assembled chains of functionalized rotating magnetic beads. *Nano Lett.* 2009; 10(2):446–451. [PubMed: 20038151]

Author Manuscript

Author Manuscript

Author Manuscript

Author Manuscript

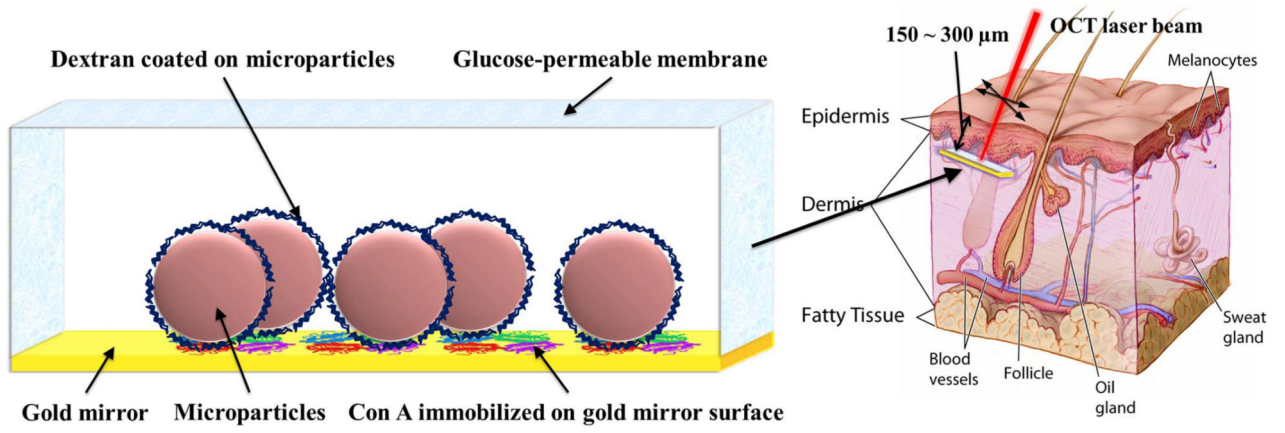


**Fig. 1.**

Illustration of the sensing element construction and implantation position. The picture of skin anatomy on the right is from National Cancer Institute (for free reuse), <http://visualsonline.cancer.gov/details.cfm?imageid=4604>.



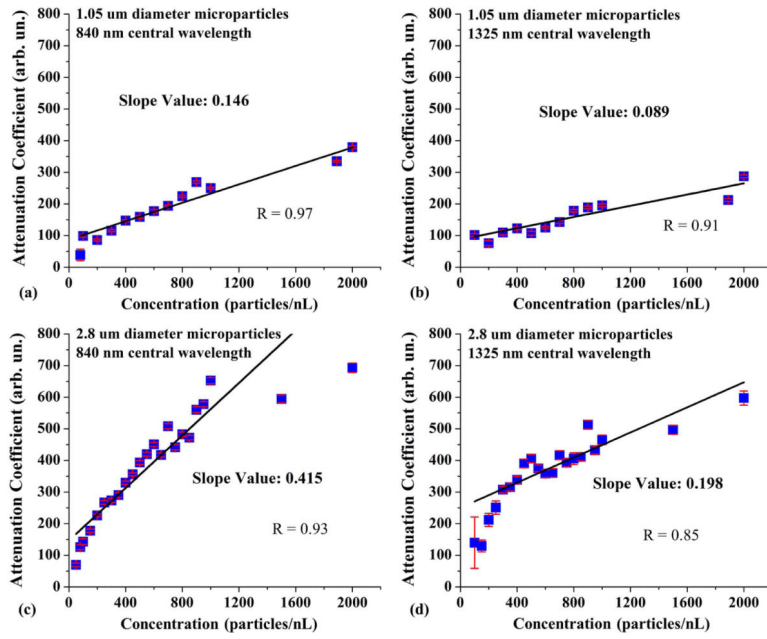


**Fig. 2.**

Attenuation coefficient of (a) 1.05  $\mu\text{m}$  diameter microparticles measured with 840 nm central wavelength OCT system, (b) 1.05  $\mu\text{m}$  diameter microparticles measured with 1325 nm central wavelength OCT system, (c) 2.8  $\mu\text{m}$  diameter microparticles measured with 840 nm central wavelength OCT system, and (d) 2.8  $\mu\text{m}$  diameter microparticles measured with 1325 nm central wavelength OCT system.  $N = 50$  for the times of measurements presented in (a), (b), (c) and (d).

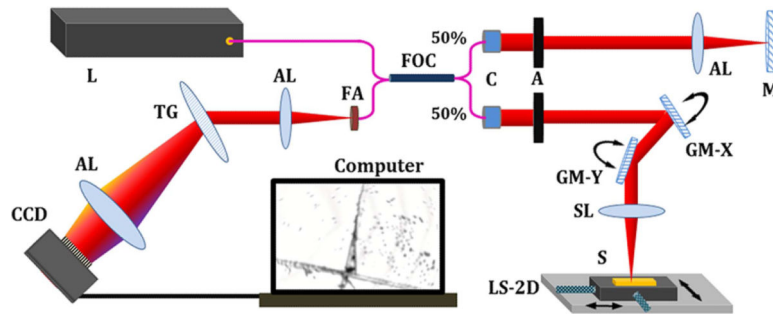


**Fig. 3.** Schematic of the spectral domain OCT system used for microparticles monitoring; L-laser, FOC-fiber optic coupler, FA-fiber adaptor, AL-achromatic lens, TG-transmission grating, C-collimator, A-aperture, M-mirror, GM-X/Y-Galvo mirror-X/Y, SL-scan lens, S-sample, LS-2D-linear stage-two-dimension.

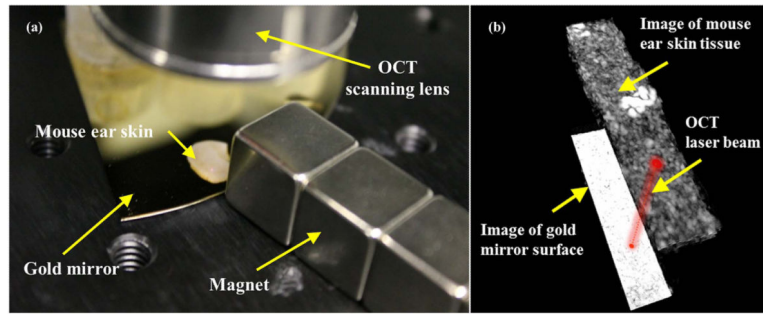


**Fig. 4.**

(a) Experimental setup for studying the OCT monitoring of microparticles' movement under mouse ear skin tissue *in vitro*. (b) Three-dimensional OCT image showing the mouse ear skin tissue and the gold mirror surface with a vertical distance of 0.7–1.0 mm between them.

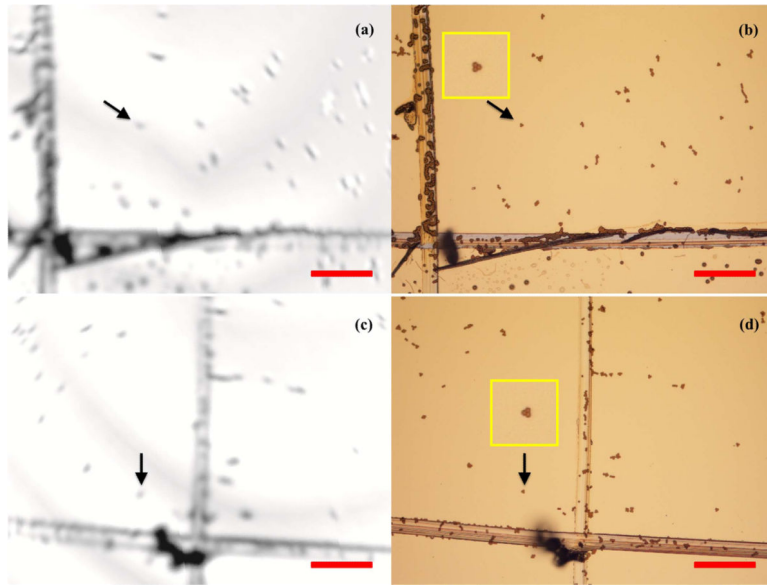


**Fig. 5.** (a) and (c) are *en face* OCT images of microparticles deposited on the gold mirror surface; (b) and (d) are the corresponding microscopic images of microparticles deposited on the gold mirror surface. The scale bars are  $100\ \mu\text{m}$  long and the black arrows point to the dark points, which correspond to the clusters of three microparticles. Partially magnified pictures from (b) and (d) are squared with yellow color.

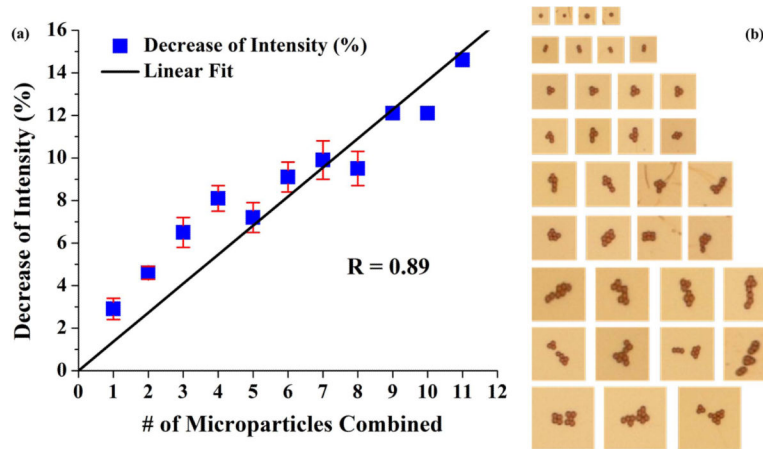


**Fig. 6.**

(a) A plot of intensity change vs. different number of microparticles in aggregates. For single microparticles and aggregates with 1–8 microparticles,  $N = 4$  (samples for measurement). For aggregates with 9, 10 and 11 microparticles,  $N = 1$  (sample for measurement). (b) Optical microscope images of microparticle aggregates used for quantifying the fractional decrease of the intensity of OCT signal.

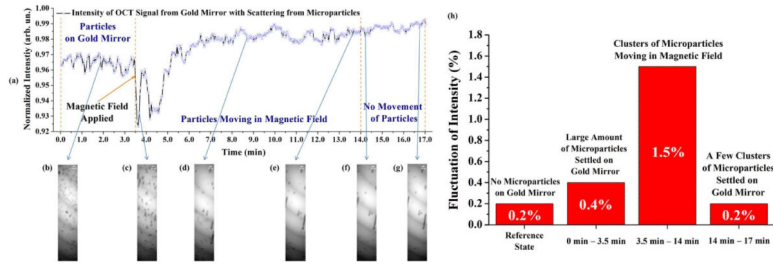


**Fig. 7.**

(a) Normalized intensity profile over time indicating the movement of microparticles on the gold mirror surface in clear media (signal normalized to the averaged intensity value with water alone). (b)–(g) En face OCT images selected from different time points. (h) The fluctuation of intensity during four periods: reference state (water alone), 0–3.5 min (before applying magnetic field), 3.5–14 min (microparticles moving in the magnetic field), and 14–17 min (clusters of microparticles left stable in the magnetic field).

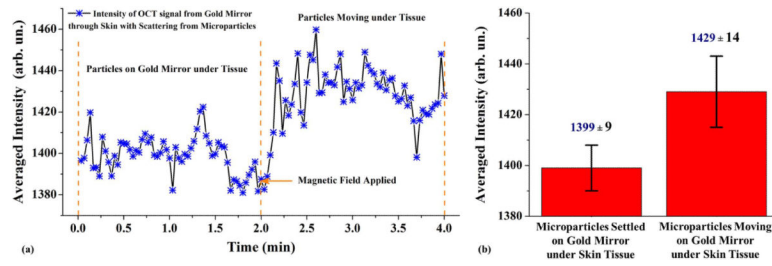


**Fig. 8.**

(a) Intensity profile over time indicating the movement of microparticles on the gold mirror surface under skin tissue *in vitro* (intensity averaged from the OCT two-dimensional scanning area). (b) Comparison of the intensity values before (0–2 min) and after (2–4 min) applying the magnetic field.